Small-Angle X-ray Scattering Study of the Pulley Effect of Slide-Ring Gels

Yuya Shinohara,*,† Kentaro Kayashima,† Yasushi Okumura,†,‡ Changming Zhao,† Kohzo Ito,†,‡ and Yoshiyuki Amemiya†,‡

Graduate School of Frontier Sciences, The University of Tokyo, 5-1-5 Kashiwanoha, Kashiwa, Chiba 277-8561, Japan, and CREST, Japan Science and Technology Agency, 4-1-8 Honcho, Kawaguchi, Saitama 332-0012, Japan

Received May 9, 2006; Revised Manuscript Received July 16, 2006

ABSTRACT: The structure of slide-ring (SR) gels in various types of solvents was investigated by small-angle X-ray scattering (SAXS). The SR gels have a unique characteristic called the "pulley effect" that the cross-links made of α-cyclodextrin molecules in a figure-eight shape can slide along the polymer chain. The SAXS results show that, in a poor solvent, the sliding cross-links form aggregates that prevent the pulley effect, while the polymer chains freely pass through the cross-links acting like pulleys in a good solvent. A vertically elliptic pattern was observed in two-dimensional SAXS profiles for covalent-bonded chemical gels in a good solvent under uniaxial horizontal deformation, while an isotropic profile was observed for the SR gels in a good solvent even under deformation. This difference in the deformation mechanism between the SR gels and the chemical gels supports the pulley effect of the SR gels.

Introduction

Supramolecules with the topological characteristics have attracted a great interest.[1−3] A typical example is provided by polyrotaxanes in which many cyclic molecules are threaded on a single polymer chain and are trapped by capping the chain with bulky end groups.[4] The polyrotaxane consisting of α-cyclodextrin and poly(ethylene glycol) (PEG) is well-known.[5−7] This architecture has been attracting attention also as a new technique for making a functional material in recent years.[8−15]

Slide-ring (SR) gel[16,17] (previously called "polyrotaxane gel") is a new type of gel synthesized by cross-linking cyclodextrins (CDs) contained in the sparse polyrotaxanes in solutions. Polymer network of SR gel consists of polymer chains with bulky end groups, and they are topologically interlocked by figure-eight cross-links of CDs. Therefore, we can classify the SR gel into "topological gel". The SR gel attracts much attention due to its unique characteristic nature, and has a high potential for many applications, such as biomaterials, cosmetic, and soft actuator. One of the remarkable characteristics of the SR gel is a "pulley effect", where the polymer chains freely pass through the cross-links, which act as pulleys. When the gel is stretched, it is assumed that the nanoscopic homogeneity in structure and stress is equalized due to the pulley effect. Characteristic structures of the SR gel have been studied by small-angle neutron scattering (SANS)[18,19] and dynamic light scattering.[20] SANS is widely used to investigate the structure of gels because the scattering length of samples can be controlled by deuteration. Furthermore, scattering length of neutron is determined by not electrons but nuclei, which makes SANS suitable to study the structure of gels composed of light elements. It is widely known that the scattering pattern of stretched gel shows characteristic anisotropic pattern, the so-called "abnormal butterfly pattern",[21−27] which has been explained by several theoretical functions proposed by Onuki[28] and by Panykov and Rabin.[29,30] The origin of the abnormal butterfly pattern is considered to be the anisotropy of nanoscopic inhomogeneity in structure that is induced by the elongation.[22] The inhomogeneity is inherent in the gelation process, and the small-angle scattering pattern of many stretched gels show the abnormal butterfly pattern.[21−27] It is, however, not the abnormal butterfly pattern but a "normal" butterfly pattern that is observed in SANS of stretched SR gels, where the normal butterfly pattern is an elliptic pattern with the long axis perpendicular to the stretching direction.[19] The results suggest that the nanoscopic inhomogeneity of the SR gels is greatly different from that of the chemical gels.

To clarify the characteristic structure of SR gels, we performed small-angle X-ray scattering (SAXS) of SR gels focusing on the structure of movable cross-links. The main advantage of SAXS over SANS is that the exposure time is shorter due to the high brilliance of synchrotron radiation X-rays. The short exposure time makes it possible to study the structure of gels in various kinds of evaporable solvents. Combination of synchrotron radiation with a two-dimensional detector that has a high sensitivity enables us to investigate the kinetics of molecular structures. Although SAXS has such advantages, few SAXS studies have been performed on the structural change of gels under elongation. This mainly results from the lack of the scattering length contrast. However, in the SAXS of the SR gels, this does not matter as will be described in this paper. We can observe the structure of SR gels from sufficient scattering by aggregates of CDs and figure-eight cross-links in addition to scattering by chain conformations. The mobile cross-links in the SR gels may lead to the formation of aggregates in a poor solvent. In this study, SAXS measurements were carried out to elucidate the nature of the pulley effect in relation to the condition of the solvent, which is expected to govern the formation of aggregates. We also measured the SAXS of the stretched SR gels in order to elucidate the role of the pulley effect in the deformation of the SR gels.

Experimental Section.

Preparation of Slide-Ring Gels and Chemical Gels. We used two types of SR gels and a chemical gel as the samples. Both types

* Corresponding author. Telephone: +81-4-7136-3751. Fax: +81-4-7136-3751. E-mail: shinohara@X-ray.k.u-tokyo.ac.jp.
† Graduate School of Frontier Sciences, The University of Tokyo.
‡ CREST, Japan Science and Technology Agency.

10.1021/ma061037s CCC: $33.50
Published on Web 09/16/2006

Table 1. Solvent Conditions and Sample Codes of Electrolyte SR Hydrogels

sample code	solvent
OH1	1 N NaOH(aq)
OH01	0.1 N NaOH(aq)
OH001	0.01 N NaOH(aq)
OH0001	0.001 N NaOH(aq)
W	water
CL0001	0.001 mol/l NaCl(aq)
CL001	0.01 mol/l NaCl(aq)
CL01	0.1 mol/l NaCl(aq)
CL1	1 mol/l NaCl(aq)

of SR gels—electrolyte SR hydrogel and neutral SR gel—are synthesized from polyrotaxanes (iAPR) composed of α-CD and poly(ethylene glycol) (MW = 35 000, Fluka) capped with 1-adamantanamine.[31] The filling rate of α-CD to a full filling state is expressed by the inclusion ratio. In fully filled polyrotaxane, a single α-CD molecule includes two ethylene glycol monomers. We defined the inclusion ratio of this polyrotaxane as 100%. We can calculate the inclusion ratio by comparing the integrations of peaks from OH groups and other hydrogen in ^{1}H NMR results because only CD molecule has hydroxyl groups.[16,31] The inclusion ratio of the SR gel used in this study was 25%. This means that our polyrotaxane contains about 100 CD rings on a PEG chain, which has about 800 ethylene glycol monomers.

Electrolyte SR Hydrogel. iAPRs (150 mg) was dissolved in 0.75 mL of 1 N sodium hydroxide (NaOH) aqueous solution at 5 °C. Cyanuric chloride (Tokyo Kasei Co.) (52.5 mg), dissolved in 1 N NaOH (0.75 mL), was dissolved in the iAPR solution to initiate the cross-linking reaction. The solution was poured into a sheet mold, 1.0 mm thick. After 5 h at room temperature, we obtained a transparent SR gel. We cut the gel sheet correctly to small rectangular samples (20 mm × 6.5 mm). We dissolved glycine (10 g) in 1 N NaOH aqueous solution (100 mL) and immersed the hydrogels in it overnight to terminate cross-linking reaction and to introduce carboxyl groups on active cross-linkers on CDs. The hydrogels were washed in a mixture of H_2O—ethanol repeatedly and then dried. We checked the weight of the dried gels, and we sorted them out so that the distribution of dry weight might become less than ±2%. The dried hydrogels samples were put into small plastic bags (30 mm × 30 mm) together with NaCl or NaOH aqueous solutions (100 μL) to make all swelling ratios almost same as grown, and the bags were heat-sealed until X-ray measurements were perfomed to avoid evaporation of the solvents. Sample codes of the electrolyte SR hydrogels are shown in Table 1. Electrolyte SR hydrogels have many carboxyl groups originating in glycine. Therefore, NaCl aqueous solution and NaOH aqueous solution are the poor solvent and the good solvent, respectively. We checked that all the samples except samples CL1 had absorbed the solvent completely before the experiment. Sample CL1 has absorbed about only 70% of the given solvent, because 1 N NaCl is strong poor solvents for the electrolyte SR hydrogel. All the SR hydrogels were transparent regardless of the solvent quality.

Neutral SR Gel. iAPRs (225 mg) was dissolved in 1.5 mL of dimethyl sulfoxide (DMSO; Wako Chemicals). Divinyl sulfone (DVS; Wako Chemicals) (100 μL) was dissolved in DMSO (1.0 mL) and was used as a cross-linker.[32] This DVS solution (150 μL) and 0.1 N NaOH aqueous solution (90 μL) were dissolved in iAPRs solution. The solution was poured into a sheet mold of 1.0 mm thickness. After 1 h at room temperature, we got a transparent SR gel. The gel sheet was cut to small rectangular samples (20 mm × 6.5 mm). The gel samples were immersed in water repeatedly to change solvent and then dried. After weight distribution was checked, the dried gel samples were put into small plastic bags (30 mm × 30 mm) together with H_2O—DMSO mixture (100 μL) to make all swelling ratios almost same as grown and heat-sealed. Their mixing volume ratios of DMSO to water in solvent were chosen to be 0 to 10, 1 to 9, 2 to 8, 3 to 7, 4 to 6, 5 to 5, 6 to 4, 7 to 3, 8 to 2, 9 to 1, and 10 to 0. Accordingly, the sample codes of neutral SR gels were defined as D0W10, D1W9, D2W8, D7W3, D6W4, D5W5, D6W4, D7W3, D8W2, D9W1, and D10W0 as shown in Table 2. We checked that all gels had absorbed all solvents before the experiment. All gels were transparent regardless of the solvent quality.

Table 2. Solvent Conditions and Sample Codes of Neutral SR Gels

sample code	vol ratio of DMSO	vol ratio of water
D0W10	0	10
D1W9	1	9
D2W8	2	8
D3W7	3	7
D4W6	4	6
D5W5	5	5
D6W4	6	4
D7W3	7	3
D8W2	8	2
D9W1	9	1
D10W0	10	0

Poly(acrylamide) Gel. Poly(acrylamide) hydrogels were used in order to compare the structure of SR hydrogels and that of covalently bonded chemical gels. The gels were prepared by free-radical cross-linking polymerization of acrylamide (AAm; Wako Chemicals) with a small amount of *N*,*N*-methylenebis(acrylamide) (BAAm; Wako Chemicals) as a cross-linker in aqueous solution. Ammonium persulfate (APS; Wako Chemicals) and *N*,*N*,*N*,*N*-tetramethylethylenediamine (TEMED; Wako Chemicals) were, respectively, the initiator and accelerator.[33] AAm (500 mg), BAAm (13.3 mg), and APS (4.0 mg) were dissolved in distilled water (10 mL). After addition of TEMED (24 μL), the solution was poured into a sheet mold, 1.0 mm thick. After 24 h at room temperature, we obtained a transparent AAm hydrogel. The gel sheet was cut into small rectangular samples (20 mm × 6.5 mm) and dried. The dried gel samples were put into small plastic bags (30 mm × 30 mm) together with H_2O (100 μL) and heat-sealed.

SAXS Experiment. SAXS experiments were performed at BL-15A, Photon Factory (Tsukuba, Japan).[34] The X-ray wavelength, λ, was 1.50 Å. As SAXS detector, an X-ray CCD detector (C4880−50−26, Hamamatsu) coupled with a 150 mm diameter X-ray Image Intensifier[35] was used. The high sensitivity of this detector enables us to obtain SAXS patterns in a few seconds. This is extremely crucial in this study because the SR gels are easily damaged by the X-ray radiation. By observing the change of SAXS patterns, we concluded that X-ray exposure (~10^{10} photons/s) of more than 60 s causes the radiation damage of the SR gels, because SAXS patterns started to change after a 60 s exposure due to the radiation damage. Therefore, we limited the exposure time to less than 10 s. Samples were placed in a uniaxial stretching machine, which was controlled from the outside of the experimental hutch. The sample-to-detector distance was around 2100 mm, which was later calibrated with a silver behenate diffraction peak.[36] In this setup, the SAXS patterns of 0.08 $nm^{-1} < q < 0.8$ nm^{-1} were recorded, where $q = 4\pi(\sin\theta)/\lambda$ is the magnitude of scattering vector and 2θ is the scattering angle.

Results and Discussion

Static Structure of SR Gels. Figure 1 shows circularly averaged SAXS intensity profiles of the electrolyte SR hydrogels on a log−log scale. The SAXS profile of OH01 is well fitted with Lorentzian function (ξ = 25 Å)

$$I_1(q) = A/(1 + \xi^2 q^2)$$

where A is the scattering intensity at $q = 0$. This clearly indicates that the polymer chains in OH01 behave as Gaussian chains. As the fraction of NaOH reduces, the scattering intensity drastically increases. To reveal the structural characteristics, we use a Kratky plot, $I(q)q^2$ vs q.[37] The scattering profile from a Gaussian chain molecule has a region at moderate angles where the scattering intensity is proportional to q^{-2} and a region at

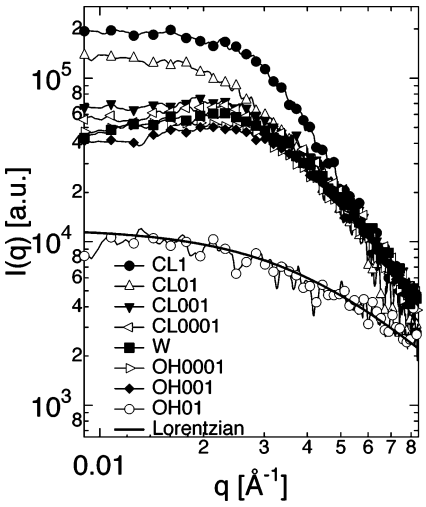

Figure 1. Circularly averaged SAXS intensity profiles of the electrolyte SR hydrogels. The line shows the fitting results of OH01 by $I_1(q)$.

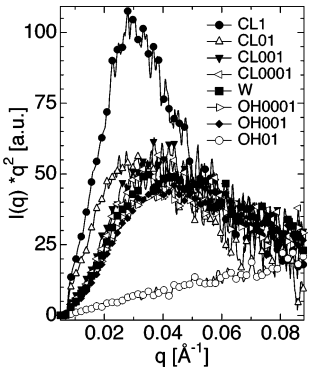

Figure 2. Kratky plot of the electrolyte SR hydrogels.

higher angles where the scattering intensity tends to be proportional to q^{-1}. The Kratky plot of such a profile shows a monotonically increasing curve with a plateau. On the other hand, the scattering profile from a globular object has a region where it obeys Porod's law, that is, $I(q) \sim q^{-4}$. Therefore, the Kratky plot of a globular object should have a peak, and its peak position should depend on the radius of gyration, R_g. Figure 2 shows Kratky plots of the Electrolyte SR hydrogels. We can clearly see the structural differences among the gels in different solvents. When the solvent is 0.1 N NaOH(aq), the scattering profile shows a monotonically increasing curve. It means that the iAPR chains in SR gels behave like Gaussian chain and that the figure-eight cross-links are not disturbing intrinsic conformation of long iAPR chains in good solvent. On the other hand, the scattering profiles on SR hydrogels absorbing the other solvents show a clear peak at around $q = 0.03$ Å^{-1}. These results indicate that the globular aggregates were formed in these solvents, and the size of aggregates is estimated to be some nanometers from the peak position in the Kratky plots. It is supposed that the electric dissociation of carboxyl groups on CDs and cross-links is suppressed at low pH, and that the repulsive force between cross-links is screened in NaCl solutions. The original iAPR without carboxyl groups is insoluble in water because of hydrogen bonds between CDs.[7] Though the inclusion ratio of CDs in the iAPR is low (25%),[31] CDs occupy more than 70% in weight ratio of dried SR hydrogel. Different from chemical gels, the figure-eight cross-links can slide freely on PEG chains to form nanoscopic aggregations without sharp entropy reduction of PEG chains. Therefore, it is surmised that the figure-eight cross-links can form aggregates easily by the hydrogen bond.

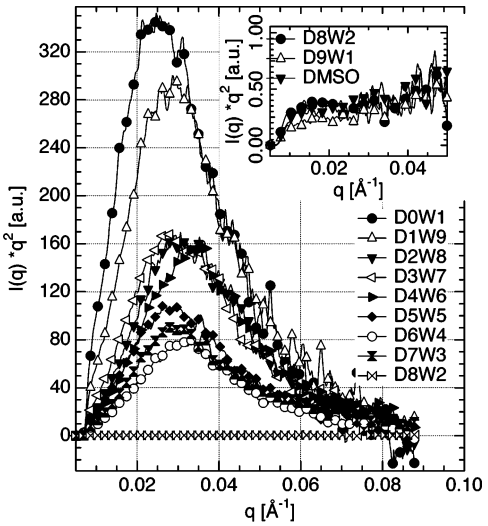

Figure 3. Kratky plot of the neutral SR gels.

This idea that the CDs form aggregate in poor solvent is supported by the difference of the solubility between CD and PEG in each solvent. We investigated the solubility of CD and PEG in each solvent. First, we dissolved PEG in 30 wt % of high concentration in 0.1 N NaOH aqueous solution, distilled water, and 0.1 mol/L NaCl aqueous solution. All the viscous solutions were clear and their viscosities were same. This result indicates that all the solutions are good solvents for PEG. Furthermore, concentration of PEG in the SR gel sample is only 2.5 wt %, and the thin PEG chains (0.3 nm) are covered with large α-CD molecules the outer diameter of which is about 1.5 nm. We can conclude that the physical interaction between PEG in SR gels is not important as the driving force to form aggregation. On the other hand, solubility of α-CD shows clear solvent dependence. The concentrations of α-CDs in the saturated solution were 13 wt % in distilled water and 0.1 mol/L NaCl aqueous solution, and 22 wt % in 0.1 N NaOH aqueous solution at room temperature. Therefore, we can conclude that the figure-eight cross-links form aggregates.

A similar structural transition on the gradation of solvent composition is observed for the neutral SR gels synthesized in DMSO. Figure 3 shows a Kratky plot of SAXS intensity profiles of the neutral SR gels. The profiles of SR gels absorbing good solvents with high DMSO ratios (100−80%) show very weak scattering intensity profiles without peaks, which are similar to those observed on the electrolyte SR hydrogel in 0.1 N NaOH. On the other hand, when the DMSO ratio becomes 70% or less, the profiles show a sudden increase of scattering intensity with a clear peak at around $q = 0.03$ Å^{-1}, the same as the results for SR hydrogels in poor solvents. Therefore, CDs form aggregates regardless of the type of SR gel.

To investigate the structural dependence on the solvent more precisely, we fit the SAXS profiles of SR gels in poor solvents with the two following functions ($I_2(q)$ and $I_3(q)$): one is the Guinier function corresponding to scattering from aggregates of CDs

$$I_2(q) = I_g \exp(-R_g^2 q^2/3)$$

where R_g is the radius of gyration of the object and Ig is the scattering intensity at $q = 0$, which is proportional to the square of aggregate volume.[37] The other function expresses the scattering due to the correlation between these aggregates

$$I_3(q) = B \exp(-C(q - q_c)^2)$$

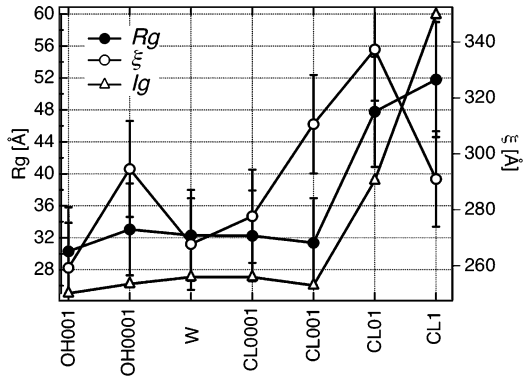

Figure 4. Dependence of the radius of gyration of the aggregates (R_g), scattering intensity at $q = 0$ (Ig) and the distance between aggregates (ξ) on the solvent of the electrolyte SR hydrogels.

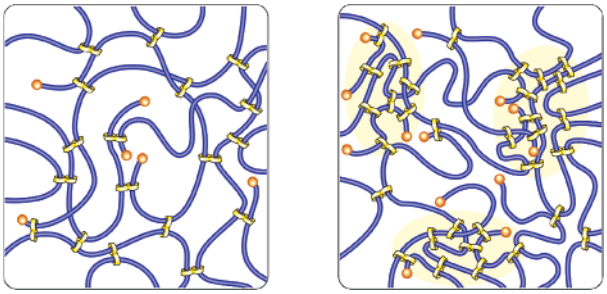

Figure 5. Schematic view of the SR gels in a poor solvent (right) and a good solvent (left). The CDs slide on polymer network to form aggregates in a poor solvent.

where $q_c = 2\pi/\xi$ and ξ is the distance between neighboring aggregates. Figure 4 shows the results of the fitting. The results show that both R_g and I_g increase by increasing the degree of poor solvent. This indicates that the repulsive force between cross-links is screened in poor solvent so that the cross-links form large aggregates when the degree of poor solvent increases. Also the distance between the aggregates increases by increasing the degree of poor solvent. It is noted that ξ in CL1 is smaller than that in CL001 and CL01. This discrepancy is considered to originate from the insufficient swelling of the gel. We added solvents of same volume (100 μL) to each sample in order to equalize the swelling ratio. However, in the case of CL1, the solvent could not be absorbed sufficiently, because the equilibrium volume in 1 N NaCl was smaller than the volume we expected to prepare. Thus, the distance between the aggregates is considered to become smaller than expected.

From the above results, we propose the model of the pulley effect of SR gels as shown in Figure 5. In a good solvent, the polymer chains freely pass through the cross-links acting like pulleys. Therefore, the SR gels are very homogeneous without higher order structure like polyrotaxanes solutions, and we could observe the polyrotaxanes behaving as a Gaussian chain. In a poor solvent, the CDs and cross-links form aggregates as shown in Figure 5, and it would become difficult for the polymers to pass through the cross-links: the pulley freezes and the pulley effect is lost.

Structure of SR Gels under Elongation. To elucidate the role of the pulley effect in the deformation of SR gels, SAXS patterns of the stretched gels were investigated. In Figure 6, SAXS patterns of the electrolyte SR hydrogels before and after elongation are shown. The stretching direction is horizontal in the figure and the elongation ratio is expressed by $\epsilon = (L + \Delta L)/L$, where L and ΔL is the initial length and the elongation length of the sample, respectively. As clearly seen, the SAXS patterns of the hydrogels before elongation are isotropic. On the other hand, at $\epsilon = 1.5$, they show abnormal butterfly patterns in poor solvents, while they show no anisotropy in a good solvent. The behavior of the scattering pattern of SR hydrogels in a poor solvent under elongation is similar to those known for the inhomogeneous chemical gel in SANS studies. The origin of the SAXS abnormal butterfly pattern can be explained by analogy with the SANS of the chemical gel. CDs of the SR gels in a poor solvent form aggregates, which leads to the formation of nonmovable cross-links. Therefore, the cross-links of the SR gels in a poor solvent behave like those of chemical gels. Thus, the SR gels in a poor solvent inherently possess the structural inhomogeneity similar to the chemical gel. The inhomogeneities are implicit in the undeformed state as CDs aggregation shown in Figure 2, but they become explicit under elongation as abnormal butterfly pattern. On the other hand, the inhomogeneities in the SR gels in a good solvent do not increase under elongation, because the polymer chains freely pass through the cross-links in a good solvent. It is noted that the relationship between the aggregate formations of cross-links and the appearance of the abnormal butterfly pattern was clearly observed in Figure 6. These results strongly suggest that the figure-eight cross-links work as pulleys in a good solvent but that they do not in a poor solvent.

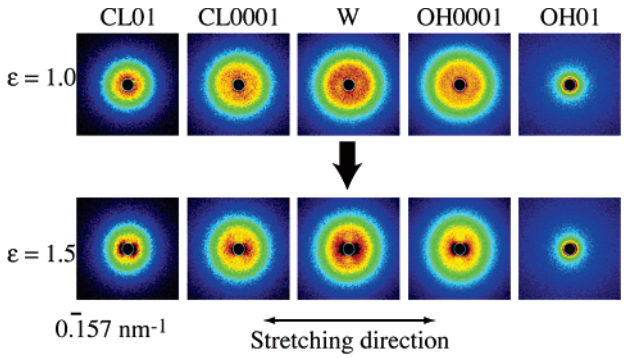

Figure 6. SAXS patterns of the electrolyte SR hydrogels in various aqueous solutions (upper) before elongation and (lower) after elongation. OH01 shows an isotropic pattern while the others show butterfly patterns.

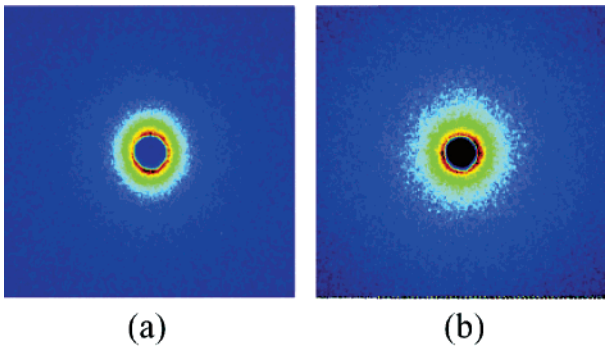

Figure 7. SAXS patterns of (a) the stretched AAm gels and (b) the stretched SR gels in a good solvent. The sample is elongated horizontal direction in the images and the stretching ratio, e, is 1.5.

Comparison of the Structure with Chemical Gels. Next we compare the 2D-SAXS patterns of the SR gels with that of chemical gel in a good solvent. Figure 7 shows the SAXS patterns of the AAm gels and the SR hydrogels in a good solvent. The gels are stretched horizontally ($\epsilon = 1.5$). The SAXS of the SR gel shows no anisotropy as shown before. On the other hand, the SAXS of the AAm gel shows an elliptic pattern with its long axis perpendicular to the stretching direction (ellipticity ~ 1.2). This scattering pattern indicates that the form factor of polymer chains is deformed under the elongation. The

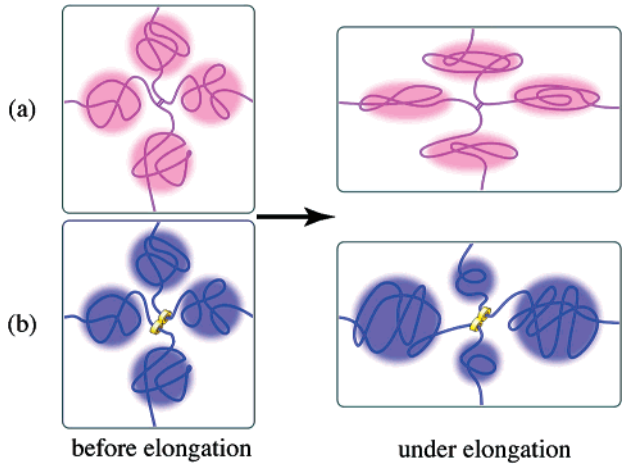

Figure 8. Schematic model of the structural change of (a) chemically bonded gels and (b) SR gels in a good solvent under elongation.

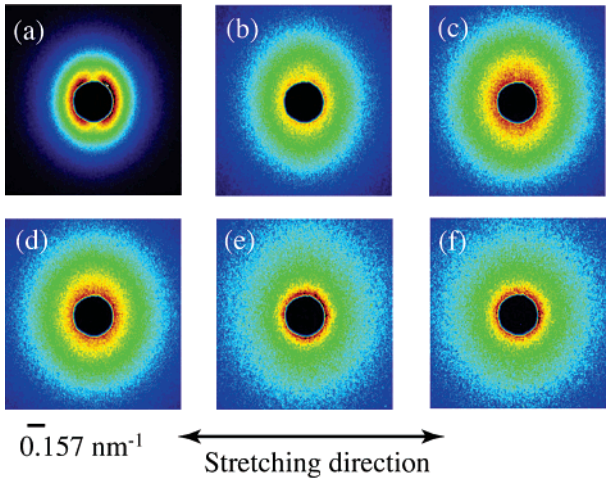

Figure 9. SAXS patterns of the stretched SR hydrogels. The stretching direction is along the horizontal axis and the stretching ratio, ϵ, is 2. Sample was (a) CL1, (b) CL001, (c) W, (d) OH001, (e) OH01, and (f) OH1.

vertically elliptic pattern corresponds to the horizontally elongated polymer chains.

Deformation Model of SR Gels under Elongation. As shown in Figure 7, the 2D-SAXS pattern of the AAm gel in a good solvent shows a vertically elliptic pattern, while that of the SR hydrogel in a good solvent shows an isotropic pattern. This difference can be explained by the following model (Figure 8). In the AAm gel, the cross-links are covalently bonded and they cannot move with respect to the polymer chains by deformation. Therefore, when the gel is stretched, the polymer chains connecting the cross-links in the direction parallel to the elongation are stretched parallel to the elongation while those connecting the cross-links vertically are compressed in the direction perpendicular to the elongation. Thus, the polymers are deformed as shown in the Figure 8a, which leads to the vertically elliptic SAXS pattern. On the other hand, the polymer chains of the SR gel freely pass through the cross-links due to the pulley effect, when the gel is stretched. Therefore, the tension at the horizontally stretched parts and the vertically compressed parts of polymers can be equilibrated by the interchange of the chains passing through the cross-links to maximize the entropy. Thus, the polymers of the SR gel in a good solvent maintain an isotropic structure even under elongation.

This model is supported by the SAXS patterns of SR gels in various solvents. Figure 9 shows the SAXS patterns of the electrolyte SR hydrogels under horizontal elongation, where the larger beam stop was used to hide the abnormal butterfly patterns in a lower q range. The SAXS patterns of the SR gel in a poor solvent shows vertically elliptic pattern while those in a good solvent show isotropic pattern. These results are explained as follows. In a poor solvent, CDs aggregates and the cross-links are no longer movable, making the pulley effect inactive. The situation is similar to that for the covalently bonded chemical gels. Therefore, the form factor of polymer chains is deformed in the same way as that of the chemical gels when stretched. This deformation should cause the elliptic SAXS patterns with its long axis perpendicular to the stretching direction.

Conclusion

Structure of the SR gels and the pulley effect is investigated by 2D-SAXS. In a good solvent, the polymer chains of the SR gel freely pass through the cross-links that act like pulleys. When the SR gel in a good solvent is stretched, it shows isotropic SAXS patterns due to the pulley effect. On the other hand, the cross-links form aggregates in a poor solvent and the pulley effect becomes inactive. The stretched SR gel in a poor solvent shows similar SAXS patterns to those of the chemical gels. Thus, we have succeeded in elucidating the behavior of the pulley effect of the SR gel in various solvents.

Acknowledgment. This study is supported by Core Research for Evolutional Science and Technology (CREST), Japan Science and Technology Agency. SAXS experiments were performed at Photon Factory with the approval of the Photon Factory Program Advisory Committee (Proposal No. 03G293).

References and Notes

(1) Wenz, G. *Angew. Chem., Int. Ed.* **1994,** *33*, 803−822.
(2) Philp, D.; Stoddart, J. F. *Angew. Chem., Int. Ed.* **1996,** *35*, 1155−1196.
(3) Gibson, H. W.; Marand, H. *Adv. Mater.* **1993,** *5*, 11−21.
(4) Wenz, G.; Keller, B. *Angew. Chem., Int. Ed.* **1992,** *31*, 197−199.
(5) Harada, A.; Kamachi, M. *Macromolecules* **1990,** *23*, 2821−2823.
(6) Harada, A.; Li, J.; Kamachi, M. *Nature (London)* **1992,** *356*, 325−327.
(7) Harada, A.; Li, J.; Kamachi, M. *J. Am. Chem. Soc.* **1994,** *116*, 3192−3196.
(8) Harada, A. *Acc. Chem. Res.* **2001,** *34*, 456−464.
(9) Li, J.; Harada, A.; Kamachi, M. *Polym. J.* **1994,** *26*, 1019−1026.
(10) Okumura, Y.; Ito, K.; Hayakawa, R. *Phys. Rev. Lett.* **1998,** *80*, 5003−5006.
(11) Fujita, H.; Ooya, T.; Yui, N. *Macromolecules* **1999,** *32*, 2534−2541.
(12) Ikeda, T.; Ooya, T.; Yui, N. *Macromol. Rapid Commun.* **2000,** *21*, 1257−1262.
(13) Okumura, Y.; Ito, K.; Hayakawa, R.; Nishi, T. *Langmuir* **2000,** *16*, 10278−10280.
(14) Ichi, T.; Watanabe, J.; Ooya, T.; Yui, N. *Biomacromolecules* **2001,** *2*, 204−210.
(15) Takata, T. *Polym. J.* **2006,** *38*, 1−20.
(16) Okumura, Y.; Ito, K. *Adv. Mater.* **2001,** *13*, 485−487.
(17) Granick, S.; Rubinstein, M. *Nat. Mater.* **2004,** *3*, 586−587.
(18) Karino, T.; Okumura, Y.; Ito, K.; Shibayama, M. *Macromolecules* **2004,** *37*, 6177−6182.
(19) Karino, T.; Okumura, Y.; Zhao, C. M.; Kataoka, T.; Ito, K.; Shibayama, M. *Macromolecules* **2005,** *38*, 6161−6167.
(20) Zhao, C. M.; Domon, Y.; Okumura, Y.; Okabe, S.; Shibayama, M.; Ito, K. *J. Phys. Cond. Matt.* **2005,** *17*, S2841−S2846.
(21) Bastide, J.; Leibler, L. *Macromolecules* **1988,** *21*, 2647−2649.
(22) Bastide, J.; Leibler, L.; Prost, J. *Macromolecules* **1990,** *23*, 1821−1825.
(23) Mendes, E.; Lindner, P.; Buzier, M.; Boue, F.; Bastide, J. *Phys. Rev. Lett.* **1991,** *66*, 1595−1598.
(24) Zielinski, F.; Buzier, M.; Lartigue, C.; Bastide, J. *Prog. Colloid. Polym. Sci.* **1992,** *90*, 115.
(25) Rouf, C.; Bastide, J.; Pujol, J. M.; Schosseler, F.; Munch, J. P. *Phys. Rev. Lett.* **1994,** *73*, 830−833.
(26) Ramzi, A.; Zielinski, F.; Bastide, J.; Boue, F. *Macromolecules* **1995,** *28*, 3570−3587.

(27) Shibayama, M.; Kawakubo, K.; Ikkai, F.; Imai, M. *Macromolecules* **1998,** *31*, 2586−2592.
(28) Onuki, A. *J. Phys. II* **1992,** *2*, 45−61.
(29) Panyukov, S.; Rabin, Y. *Macromolecules* **1996,** *29*, 7960−7975.
(30) Rabin, Y.; Panyukov, S. *Macromolecules* **1997,** *30*, 301−312.
(31) Araki, J.; Zhao, C. M.; Ito, K. *Macromolecules* **2005,** *38*, 7524−7527.
(32) Fleury, G.; Schlatter, G.; Brochon, C.; Hadziioannou, G. *Polymer* **2005**, *46*, 8494−8501.
(33) Okay, O.; Sariisik, S. B.; Zor, S. D. *J Appl. Polym. Sci.* **1998,** *70*, 567−575.
(34) Amemiya, Y.; Wakabayashi, K.; Hamanaka, T.; Wakabayashi, T.; Matsushita, T.; Hashizume, H. *Nucl. Instrum. Methods Phys. Res.* **1983,** *208*, 471−477.
(35) Amemiya, Y.; Ito, K.; Yagi, N.; Asano, Y.; Wakabayashi, K.; Ueki, T.; Endo, T. *Rev. Sci. Instrum.* **1995,** *66*, 2290−2294.
(36) Blanton, T. N.; Barnes, C. L.; Lelental, M. *J. Appl. Crystallogr*. **2000,** *33*, 172−173.
(37) Glatter, O.; Kratky, O. *Small-Angle X-ray Scattering*; Academic Press: London, 1982.

MA061037S